

Communication

## A Fast Colourimetric Assay for Lead Detection Using Label-Free Gold Nanoparticles (AuNPs)

Guowei Zhong <sup>1</sup>, Jinxia Liu <sup>1,\*</sup> and Xinyu Liu <sup>2,\*</sup>

<sup>1</sup> Department of Civil Engineering, McGill University, Montreal, QC H3A 0C3, Canada;  
E-Mail: guowei.zhong@mail.mcgill.ca

<sup>2</sup> Department of Mechanical Engineering, McGill University, Montreal, QC H3A 0C3, Canada

\* Authors to whom correspondence should be addressed; E-Mails: jinxia.liu@mcgill.ca (J.L.); xinyu.liu@mcgill.ca (X.L.); Tel.: +1-514-398-7938 (J.L.); +1-514-398-1526 (X.L.).

Academic Editor: Fan-Gang Tseng

Received: 31 December 2014 / Accepted: 15 April 2015 / Published: 22 April 2015

---

**Abstract:** A sensitive colourimetric method for lead (Pb<sup>II</sup>) detection is reported in this paper using a common tripeptide, glutathione (GSH), and label-free gold nanoparticles (AuNPs). A limit of detection of 6.0 ppb in water was achieved and the dynamic linear range was up to 500 ppb. Selectivity over fourteen potential interfering metal ions was tested and most of these metal ions do not interfere with the method.

**Keywords:** gold nanoparticle; label-free; lead; glutathione; colourimetric assay

---

### 1. Introduction

Lead is known for being highly toxic, carcinogenic and bioaccumulative [1]. One of the well-recognized major exposure routes to human is through the drinking water provided by municipal water treatment plants [2]. The World Health Organization (WHO), the Health Canada and the United States Environmental Protection Agency (U.S. EPA) have issued guidelines or standards on lead in drinking water, setting the upper permissible limit at 10 ppb, 10 ppb and 15 ppb, respectively [3–5]. These limits demand high performance on analytical methods for lead detection, such that only those which have sufficient sensitivity can be applied. Analytical techniques such as atomic absorption spectrometry and inductively-coupled plasma atomic emission spectrometry are frequently used since they provide limits of detection (LOD) as low as 1 ppb for lead. However, these techniques require highly sophisticated equipment and costly consumables [6]. As they are limited by the bulky

equipment and the need for highly skilled analysts, these analytical techniques are not suitable for on-site applications [7]. Therefore, there is a great demand for developing low-cost, simple and sufficiently sensitive detection methods, which can supplement or even replace the conventional methods. A recent event that highlights the need for rapid and low-cost lead detection method is the incidence of elevated lead levels in the drinking water system of Washington, D.C. area in the USA, where about a million population had been exposed to lead levels higher than the US drinking water standards for almost 4 years [8,9]. Not only in developed countries, but also in developing ones, a broader application of such sensitive and cost-efficient sensor is highly desirable.

Gold nanoparticles (AuNPs), among the crucial and versatile materials in nanotechnology [10], have been widely applied in many applications, such as cancer diagnosis [11], drug delivery [12], bio-sensing [13], and environmental monitoring [14–17]. The wide use of AuNPs is mainly attributed to their unique surface chemistry and optical properties. Several researchers have developed assays to utilize functionalized or modified AuNPs as sensors for environmental monitoring of heavy metal ions in water, and LODs as low as 10 ppb have been reported. For instance, nucleotide-based sensors coupled with AuNPs have been shown to be highly sensitive and selective [18–21]; however, stringent preservation conditions (such as very low temperature), complex procedures, and the need for high-sensitivity fluorescence measurement for these sensors greatly limited the integration of the assays onto lab-on-a-chip systems and the use for on-site applications. Others have developed protein-based AuNP sensor, which required less pretreatment of AuNPs. However, finalizing the functional AuNPs still required at least 24 h before use [22,23]. Huang *et al.* [24] and D'Agostino *et al.* [21] have respectively used gallic acid and glutathione (GSH) as surface modifiers for detection of lead, yet the equilibration time (20–60 min) was still a limit for fast screening. Chai *et al.* [25], Mao *et al.* [26] and Chu *et al.* [27] have used GSH-modified AuNPs as sensors for heavy metal detection, but the shelf-life of such sensors was short and intended functions could be rapidly lost.

In the present study, we developed a rapid and sensitive Pb<sup>II</sup> assay that used label-free AuNPs, hence avoiding the modification process and greatly simplifying reagent storage as well as operations. Unlike other approaches that required prior synthesis of specific peptides [6,28], our method directly utilized a common peptide, GSH, which can bind to AuNPs and coordinate with Pb<sup>II</sup> at the same time (Figure 1). AuNPs were used as a label-free colourimetric reporter and glutathione (GSH) as a linker that selectively binds to Pb<sup>II</sup> ions and thus recognizes the metal ion. The working principle, detection limit, dynamic range, and selectivity of the method are discussed herein.

## 2. Materials and Methods

### 2.1. Materials and Gold Nanoparticle Preparation

Gold (III) chloride trihydrate (HAuCl<sub>4</sub>, 99.9%), ethylenediamine tetraacetic acid disodium salt (EDTA, ≥99.0%) and GSH (L-Glutathione reduced, ≥98.0%) were obtained from Sigma-Aldrich (Ontario, Canada). Potassium phosphate monobasic (ACS), dibasic anhydrous (ACS), sodium citrate dihydrate (≥99%) and sodium chloride (NaCl, ACS) were obtained from Fisher Scientific (Ontario, Canada). All certified metal ion solutions (Ca<sup>II</sup>, As<sup>III</sup>, Mg<sup>II</sup>, Hg<sup>II</sup>, Cu<sup>II</sup>, Ni<sup>II</sup>, Fe<sup>III</sup>, Ba<sup>II</sup>, Co<sup>II</sup>, Ag<sup>I</sup>, Mn<sup>II</sup>,

$\text{Cd}^{\text{II}}$ ,  $\text{Zn}^{\text{II}}$ ,  $\text{Cr}^{\text{III}}$ ,  $\text{Al}^{\text{III}}$ ) were obtained either from Sigma-Aldrich or Fisher Scientific. Deionized water was also purchased from Fisher Scientific.

The AuNPs were synthesized using the classic Turkevich–Frens method [29,30] and the protocol developed by Liu and Lu [31]. AuNPs were imaged via transmission electron microscopy (TEM) using a Tecnai GF20 system (FEI, Hillsboro, OR, USA) operated at 200 keV.

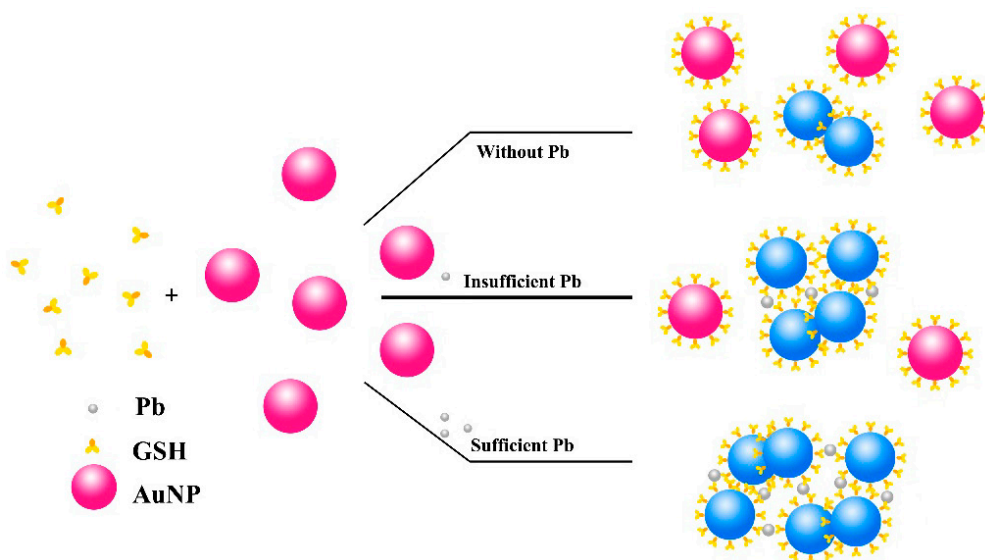


**Figure 1.** Schematic principle of the time-dependent determination of  $\text{Pb}^{\text{II}}$  concentrations in water. The aggregation rate of AuNPs varies according to concentrations of  $\text{Pb}^{\text{II}}$ .

## 2.2. Assay

The assay for detection of  $\text{Pb}^{\text{II}}$  in water was conducted by monitoring the aggregation behavior of the AuNPs in the presence of GSH, and corresponding changes in absorbance of the assay solutions were measured using a spectrophotometer (SpectraMax M5, Molecular Devices, Sunnyvale, CA, USA). The assay was performed in clear-bottom 96-well plates (Costar<sup>®</sup>). The GSH solution was freshly prepared in the presence of a background electrolyte (NaCl) and a potassium phosphate buffer. The assay was initiated by mixing 150  $\mu\text{L}$  of a water sample with 50  $\mu\text{L}$  of the GSH solution, followed by addition of 100  $\mu\text{L}$  of the AuNP aqueous solution ( $\sim 13$  nM) [31]. The final concentrations of NaCl, GSH and the phosphate buffer (pH = 8) in the 300  $\mu\text{L}$  assay solution were 10, 4.1, and 2.6 mM, respectively.

The concentrations of NaCl, GSH and phosphate buffer were tested prior to optimizing the assay. After sufficient mixing via pipetting was performed, the assay solution was maintained at room temperature for 2 min. The absorbance of the assay solution was then recorded at wavelengths of 520 nm and 610 nm every minute, for a total of 15 min. A spectrum scan ranging from 480 to 680 nm was also recorded. The time profile of the absorbance ratio at two wavelengths ( $A_{610}/A_{520}$ ) was reconstructed using Microsoft Excel 2013.

### 3. Results and Discussion

#### 3.1. Gold Nanoparticles

The average size of AuNPs used in the assay was measured to be  $15.2 \text{ nm} \pm 3.6 \text{ nm}$  (Figure S1a in supplementary materials). The AuNP solution had a characteristic surface plasma resonance peak at 520 nm and bright ruby-red colour (Figure S1b in supplementary materials). The uniformity of AuNP sizes is essential for achieving high quality of optical performance, thus high selectivity and sensitivity of the detection method. The AuNP solution can be stored at 4 °C for an extended period time (>3 months) without losing their properties and be readily used for  $\text{Pb}^{\text{II}}$  assay.

#### 3.2. Mechanism, Assay Optimization and Performance

GSH is a non-protein tri-peptide with a gamma peptide linkage between the amine group of cysteine and the carboxyl group of the glutamate side-chain, and it can cause aggregation of AuNPs. The thiol group (–SH) of the cysteinyl residue has a high affinity towards gold and Au–S covalent bond formation is expected when GSH is present in AuNPs suspension [32]. Simultaneously, GSH molecules form intermolecular hydrogen bonding among themselves, even when the GSH molecules are adsorbed to the surfaces of AuNPs. Therefore, the combination of such molecular interactions enables GSH to aggregate AuNPs under certain conditions [33]. GSH-mediated aggregation of AuNPs progresses very slowly, probably because of the weak hydrogen bonding [33]. Lead ( $\text{Pb}^{\text{II}}$ ) can strongly induce aggregation of GSH-modified AuNPs at certain pH levels through formation of coordination complexes between  $\text{Pb}^{\text{II}}$  and the carboxyl group (–COO–), two of which are present in each GSH molecule [26,34]. The thiol group is also believed to be involved in metal-GSH complex formation. Therefore, the addition of  $\text{Pb}^{\text{II}}$  to an aqueous solution can greatly enhance the rate of AuNP aggregation in the presence of GSH, and much faster colour changes can be observed accordingly. Therefore, by precisely monitoring the progression of aggregation of AuNPs through corresponding colour change, this assay can be used to detect  $\text{Pb}^{\text{II}}$ , with high selectivity and sensitivity, as demonstrated below. As shown in Figure 2, in the presence of sufficient levels of  $\text{Pb}^{\text{II}}$ , there were substantial changes in the absorbance profile (Figure 2a) and colours (Figure 2b) of the AuNP solution in the visible spectrum as a result of AuNP aggregating, when compared to the control. For example, 1 ppm  $\text{Pb}^{\text{II}}$  led to a complete colour change of the AuNP solution from ruby red to blue within 10 min, while the colour change in the control (without the addition of  $\text{Pb}^{\text{II}}$ ) progressed much slower (Figure 2b). The colour changes at other  $\text{Pb}^{\text{II}}$  concentrations are demonstrated in Figure S2 in supplementary materials.

When the absorbance ratio recorded at 10 min was plotted again  $\text{Pb}^{\text{II}}$  concentration (Figure 3), there was a linear relationship within a range of concentrations (Figure 3b). Such relationship was used as the basis for  $\text{Pb}^{\text{II}}$  quantitation in aqueous solutions. For test conditions used in the study, a linear calibration curve ( $R^2 = 0.9929$ ) up to 500 ppb was achieved (Figure 3b insert). The limit of detection (LOD), which corresponds to the average signal of multiple blanks plus 3 times of their standard deviation, was determined to be 6.0 ppb using an EPA method [35]. The LOD was lower than the upper permissible limit of  $\text{Pb}^{\text{II}}$  in drinking water from WHO, indicating the high sensitivity of the assay.

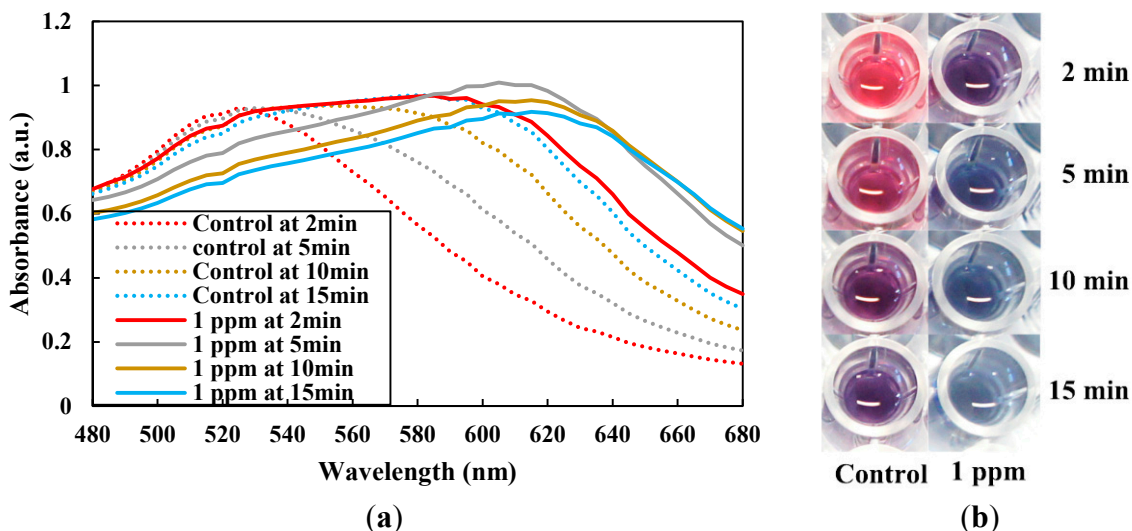


**Figure 2.** (a) Evolution of the absorbance of the control solution (dotted lines) and the solution with 1 ppm lead (solid lines) in the visible spectrum range; and (b) the solution colour changes corresponding to different incubation times.

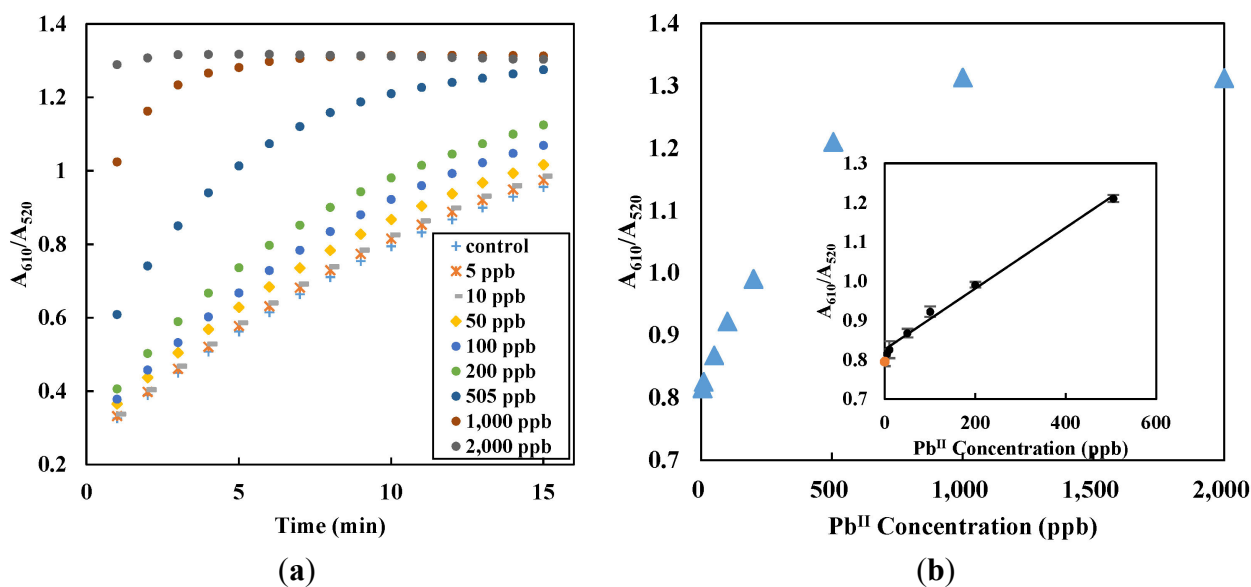


**Figure 3.** (a) Evolution of the absorbance ratio ( $A_{610}/A_{520}$ ) at 5, 10, 50, 100, 200, 505, 1000, and 2000 ppb of  $Pb^{II}$  over time; and (b) responses of different concentrations of lead standard solutions. The inserted chart demonstrates the calibration curve for the linear range of 6–500 ppb. All data were collected at 10 min and based on 4 independent measurements. The orange dot in the inserted chart represents the control without the addition of lead.

Ionic strength [6,36], GSH concentration [37], and pH are critical in controlling assay performance, colour transition of AuNP solution, and ligand-lead interaction. The influence of GSH concentration and ionic strength was investigated at a solution pH 8 and  $Pb^{II}$  concentration of 10 ppb. As shown in Figure 4, higher GSH concentrations or ionic strength in terms of NaCl concentration increased the sensitivity, expressed as  $\Delta A_{610}/A_{520}$  between control and 10 ppb  $Pb^{II}$ . At higher NaCl/GSH concentrations, aggregation of AuNP developed faster and therefore a better resolution between the

control and 10 ppb  $\text{Pb}^{\text{II}}$  could be achieved. However, NaCl/GSH concentrations must be tuned within certain limits. When AuNP aggregation occurred too rapid to allow timely measurement of colour change, sensitivity of the assay would be lost. In addition, attenuation of the plasmon resonance peak and peak flattening [36] were also observed with very high NaCl concentration (Figure S3 in supplementary materials), which showed distinct spectrum from that of GSH-induced AuNP aggregation. Characteristic colour change of the AuNP solution disappeared accordingly. Effect of pH was also investigated because pH affects not only the stability of AuNPs but also binding of  $\text{Pb}^{\text{II}}$  to GSH and AuNPs (Table S1 in supplementary materials). Higher pH has been found to suppress the undesirable interactions between GSH and AuNP through  $-\text{COOH}$  and  $\alpha$ -amines [37], allowing gradual aggregation of AuNPs to achieve the best resolution. The best resolution between the control and 10 ppb  $\text{Pb}^{\text{II}}$  was achieved by adjusting the NaCl/GSH concentration to 10 mM/4.1 mM, and using a pH 8 phosphate buffer (Figure 4).

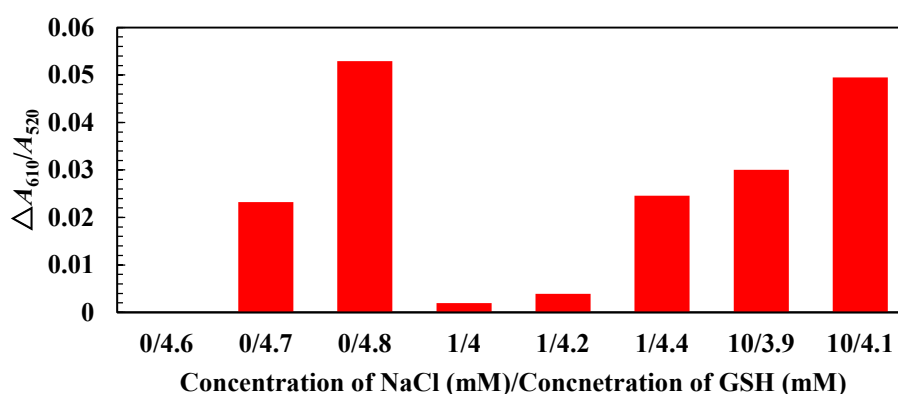


**Figure 4.** The effect of NaCl and GSH concentration on assay sensitivity ( $\Delta A_{610}/A_{520}$ ) (buffered by a pH 8 phosphate buffer solution).

### 3.3. Selectivity Evaluation

To evaluate the selectivity of the assay for metal ion  $\text{Pb}^{\text{II}}$  using label-free AuNPs, 14 metal ions ( $\text{Ca}^{\text{II}}$ ,  $\text{As}^{\text{III}}$ ,  $\text{Mg}^{\text{II}}$ ,  $\text{Hg}^{\text{II}}$ ,  $\text{Cu}^{\text{II}}$ ,  $\text{Ni}^{\text{II}}$ ,  $\text{Fe}^{\text{III}}$ ,  $\text{Ba}^{\text{II}}$ ,  $\text{Co}^{\text{II}}$ ,  $\text{Ag}^{\text{I}}$ ,  $\text{Mn}^{\text{II}}$ ,  $\text{Cd}^{\text{II}}$ ,  $\text{Zn}^{\text{II}}$ ,  $\text{Cr}^{\text{III}}$ ,  $\text{Al}^{\text{III}}$ ) were selected and tested against  $\text{Pb}^{\text{II}}$ . The same assay procedures were performed, where each metal ion was added to AuNP solutions instead of  $\text{Pb}^{\text{II}}$  to reach 1  $\mu\text{M}$ , and the absorbance ratio of  $A_{610}/A_{520}$  was recorded at the detection time of 10 min. The relative signal intensity of a particular metal ion to that of  $\text{Pb}^{\text{II}}$  at 1  $\mu\text{M}$  was calculated. As shown in Figure 5, most of those metal ions had negligible impact (no more than 9.2%) on the assay at 1  $\mu\text{M}$ , suggesting the assay is highly selective for  $\text{Pb}^{\text{II}}$  over other metal ions. The most significant interference, or the highest signal generated by other metal ions was from  $\text{Cr}^{\text{III}}$  which generated a signal about 25% of  $\text{Pb}^{\text{II}}$  (Figure 5). It was likely due to the high affinity of  $\text{Cr}^{\text{III}}$  for GSH [38]. Thus, method to minimize the impact of those interfering ions was further explored by using a masking agent—EDTA.

EDTA was chosen based on its higher formation constant with potential interfering ions than with  $\text{Pb}^{\text{II}}$  [39–41]. The formation constant of EDTA– $\text{Cr}^{\text{III}}$  and EDTA– $\text{Pb}^{\text{II}}$  were reported to be  $-23.4$  and  $-18$ , respectively [42]. The test was conducted by examining the impact of EDTA on  $\text{Pb}^{\text{II}}$  (1  $\mu\text{M}$ ) or  $\text{Cr}^{\text{III}}$  (4  $\mu\text{M}$ ), as well as on a mixed solution containing both ions. As shown in Figure 6, 1  $\mu\text{M}$  EDTA

could effectively and specifically mask  $\text{Cr}^{\text{III}}$  while having little influence on  $\text{Pb}^{\text{II}}$ . The signal response in the presence of all three species ( $\text{Pb}^{\text{II}}$ ,  $\text{Cr}^{\text{III}}$  and EDTA) was only slightly higher (~10%) than the response from 1  $\mu\text{M}$   $\text{Pb}^{\text{II}}$  alone. It was noted that the increase in signal response was not proportional to the increase in concentration of  $\text{Cr}^{\text{III}}$ . The presence of 4  $\mu\text{M}$   $\text{Cr}^{\text{III}}$  in a solution with 1  $\mu\text{M}$   $\text{Pb}^{\text{II}}$  caused a signal response that was about three times of the response from 1  $\mu\text{M}$   $\text{Pb}^{\text{II}}$  alone. It might be due to accelerated AuNP aggregation at higher ion concentrations. The presence of  $\text{Pb}^{\text{II}}$  and  $\text{Cr}^{\text{III}}$  in real samples at such concentrations, especially in drinking water, is probably very rare. Therefore, this method has the potential for the analysis of real water samples.

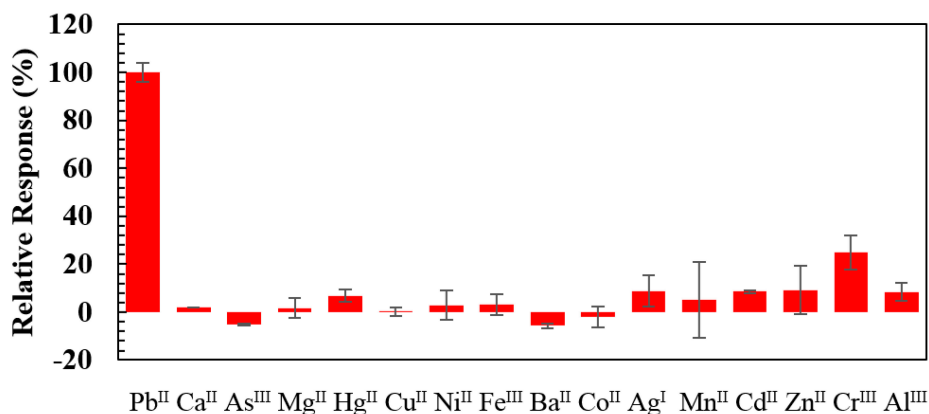


**Figure 5.** Selectivity test of the  $\text{Pb}^{\text{II}}$  detection method showing the relative response of each metal ion with respect to  $\text{Pb}^{\text{II}}$  (set as 100%). Fourteen interfering ions were tested in the presence of 1.0  $\mu\text{M}$  each and the error bars represent the standard deviation of four replicates.

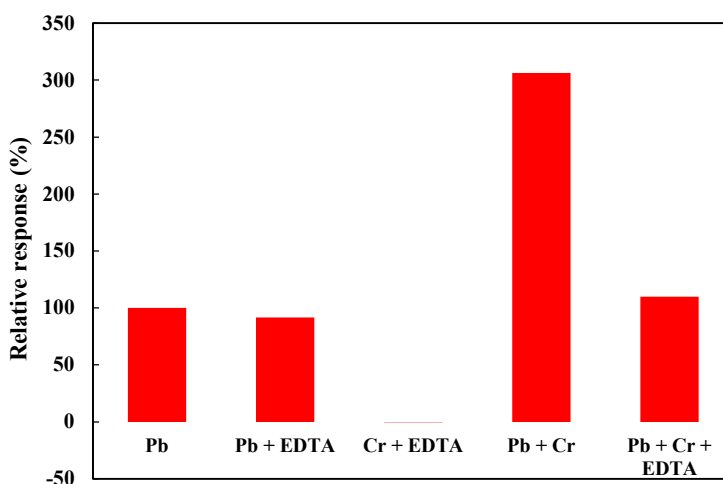


**Figure 6.** Improvement of the selectivity in by the addition of EDTA as a masking agent ( $\text{Pb}^{\text{II}}$  was at 1  $\mu\text{M}$ ,  $\text{Cr}^{\text{III}}$  4  $\mu\text{M}$  and EDTA 1  $\mu\text{M}$ ).

Further use of the assay for  $\text{Pb}^{\text{II}}$  detection in drinking water with high hardness is currently being tested. We are investigating chemical routes to minimize the effect of other potential interfering ions, in particular  $\text{Ca}^{\text{II}}$  and  $\text{Mg}^{\text{II}}$ , which could be present at much higher levels than what we have tested in the present study. That requires fine tuning solution pH, ionic strength, and likely masking agents to find conditions that favor high  $\text{Pb}^{\text{II}}$  selectivity and rapid AuNP aggregation. Although both  $\text{Pb}^{\text{II}}$  and

Ca<sup>II</sup> ions are classified as “hard” metal and binds to GSH via similar oxygen donors, they form different types of complexes with GSH, which has eight possible coordination sites [43]. In addition, a better understanding of the coordination chemistry of AuNPs with GSH or other ligands merits further investigation for improving AuNP-based sensors for heavy metal detection.

#### 4. Conclusions

In conclusion, a rapid label-free assay using AuNPs for sensitive Pb<sup>II</sup> detection in water has been demonstrated without the use of corrosive or hazardous agents. The LOD of this assay conducted using deionized water spiked with Pb<sup>II</sup> was 6.0 ppb, lower than the WHO limit for drinking water of 10 ppb. The current assay provided a short detection time of 10 min and a linear dynamic range of 6–500 ppb, and can be easily implemented using a spectrophotometer. Without the need for prior modification of AuNPs, the assay has a great potential for field applications. In fact, the assay has been recently realized in a portable lab-on-a-chip system, which includes a custom-made colourimetric reader for signal readout [44]. Such system intended for field applications can greatly benefit from such assay that is not limited by stringent preservation requirements.

#### Acknowledgments

The authors thank the Fonds de recherche du Québec-Nature et Technologies (FQRNT) and the Natural Sciences and Engineering Research Council of Canada (NSERC) for the financial support of this research.

#### Author Contributions

Guowei Zhong, Jinxia Liu, and Xinyu Liu designed the research. Guowei Zhong performed experiments and analyzed data. Guowei Zhong, Jinxia Liu, and Xinyu Liu prepared the manuscript.

#### Supplementary Materials

Supplementary materials including Table S1 and Figures S1–S3 can be accessed at: <http://www.mdpi.com/2072-666X/6/4/462/s1>.

#### Conflicts of Interest

The authors declare no conflict of interest.

#### References

1. Madejón, P.; Murillo, J.M.; Marañón, T.; Cabrera, F.; López, R. Bioaccumulation of As, Cd, Cu, Fe and Pb in wild grasses affected by the aznalcóllar mine spill (SW Spain). *Sci. Total Environ.* **2002**, *290*, 1–3.
2. Bowen, W.H. Exposure to metal ions and susceptibility to dental caries. *J. Dent. Educ.* **2001**, *65*, 1046–1053.

3. World Health Organization. *Guidelines for Drinking-Water Quality*, 3rd ed.; WHO Press: Geneva, Switzerland, 2008; Volume 1.
4. Health Canada. *Guidelines for Canadian Drinking Water Quality Summary Table*; Health Canada: Ottawa, ON, Canada, 2012.
5. U.S. Environmental Protection Agency. *National Primary Drinking Water Regulations*; EPA 816-F-09-004; U.S. EPA: Washington, DC, USA, 2009.
6. Xia, N.; Shi, Y.F.; Zhang, R.C.; Zhao, F.; Liu, F.; Liu, L. Simple, rapid and label-free colourimetric assay for arsenic based on unmodified gold nanoparticles and a phytochelatin-like peptide. *Anal. Methods* **2012**, *4*, 3937–3941.
7. Gao, A.R.; Liu, X.; Li, T.; Zhou, P.; Wang, Y.L.; Yang, Q.; Wang, L.H.; Fan, C.H. Digital microfluidic chip for rapid portable detection of mercury(II). *IEEE Sens. J.* **2011**, *11*, 2820–2824.
8. Guidotti, T.L.; Calhoun, T.; Davies-Cole, J.O.; Knuckles, M.E.; Stokes, L.; Glymph, C.; Lum, G.; Moses, M.S.; Goldsmith, D.F.; Ragain, L. Elevated lead in drinking water in Washington, DC, 2003–2004: The public health response. *Environ. Health Perspect.* **2007**, *115*, 695–701.
9. U.S. Environmental Protection Agency. *Elevated Lead in D.C. Drinking Water: A Study of Potential Causative Events*; EPA 810-F-07-002; U.S. EPA: Washington, DC, USA, 2007.
10. Amendola, V.; Meneghetti, M. Size evaluation of gold nanoparticles by UV–Vis spectroscopy. *J. Phys. Chem. C* **2009**, *113*, 4277–4285.
11. Huang, X.; Jain, P.K.; El-Sayed, I.H.; El-Sayed, M.A. Gold nanoparticles: Interesting optical properties and recent applications in cancer diagnostics and therapy. *Future Med.* **2007**, *2*, 681–693.
12. Bao, Q.Y.; Geng, D.D.; Xue, J.W.; Zhou, G.; Gu, S.Y.; Ding, Y.; Zhang, C. Glutathione-mediated drug release from tiopronin-conjugated gold nanoparticles for acute liver injury therapy. *Int. J. Pharm.* **2013**, *446*, 112–118.
13. Wang, Z.; Lu, Y. Functional DNA directed assembly of nanomaterials for biosensing. *J. Mater. Chem.* **2009**, *19*, 1788–1798.
14. Li, J.; Lu, Y. A highly sensitive and selective catalytic DNA biosensor for lead ions. *J. Am. Chem. Soc.* **2000**, *122*, 10466–10467.
15. Zhang, M.; Liu, Y.Q.; Ye, B.C. Colourimetric assay for parallel detection of Cd<sup>2+</sup>, Ni<sup>2+</sup> and Co<sup>2+</sup> using peptide-modified gold nanoparticles. *Analyst* **2012**, *137*, 601–607.
16. Darbha, G.K.; Singh, A.K.; Rai, U.S.; Yu, E.; Yu, H.; Chandra Ray, P. Selective detection of mercury (II) ion using nonlinear optical properties of gold nanoparticles. *J. Am. Chem. Soc.* **2008**, *130*, 8038–8043.
17. Huang, D.; Niu, C.; Ruan, M.; Wang, X.; Zeng, G.; Deng, C. Highly sensitive strategy for Hg<sup>2+</sup> detection in environmental water samples using long lifetime fluorescence quantum dots and gold nanoparticles. *Environ. Sci. Technol.* **2013**, *47*, 4392–4398.
18. Wang, Z.; Lee, J.H.; Lu, Y. Label-free colourimetric detection of lead ions with a nanomolar detection limit and tunable dynamic range by using gold nanoparticles and dnzyme. *Adv. Mater.* **2008**, *20*, 3263–3267.
19. Liu, J.; Lu, Y. Adenosine-dependent assembly of aptazyme-functionalized gold nanoparticles and its application as a colourimetric biosensor. *Anal. Chem.* **2004**, *76*, 1627–1632.
20. Hui, W.; Bingling, L.; Jing, L.; Shaojun, D.; Erkang, W. Dnzyme-based colourimetric sensing of lead (Pb<sup>2+</sup>) using unmodified gold nanoparticle probes. *Nanotechnology* **2008**, *19*, 095501.

21. D'Agostino, A.; Taglietti, A.; Bassi, B.; Donà, A.; Pallavicini, P. A naked eye aggregation assay for Pb<sup>2+</sup> detection based on glutathione-coated gold nanostars. *J. Nanopart. Res.* **2014**, *10*, 1–11.
22. Guo, Y.; Wang, Z.; Qu, W.; Shao, H.; Jiang, X. Colourimetric detection of mercury, lead and copper ions simultaneously using protein-functionalized gold nanoparticles. *Biosens. Bioelectron.* **2011**, *26*, 4064–4069.
23. Lin, Y.-W.; Huang, C.-C.; Chang, H.-T. Gold nanoparticle probes for the detection of mercury, lead and copper ions. *Analyst* **2011**, *136*, 863–871.
24. Huang, K.W.; Yu, C.J.; Tseng, W.L. Sensitivity enhancement in the colourimetric detection of lead(II) ion using gallic acid-capped gold nanoparticles: Improving size distribution and minimizing interparticle repulsion. *Biosens. Bioelectron.* **2010**, *25*, 984–989.
25. Chai, F.; Wang, C.; Wang, T.; Li, L.; Su, Z. Colourimetric detection of Pb<sup>2+</sup> using glutathione functionalized gold nanoparticles. *ACS Appl. Mater. Interfaces* **2010**, *2*, 1466–1470.
26. Mao, X.; Li, Z.-P.; Tang, Z.-Y. One pot synthesis of monodispersed L-glutathione stabilized gold nanoparticles for the detection of Pb<sup>2+</sup> ions. *Front. Mater. Sci.* **2010**, *5*, 322–328.
27. Chu, W.; Zhang, Y.; Li, D.; Barrow, C.J.; Wang, H.; Yang, W. A biomimetic sensor for the detection of lead in water. *Biosens. Bioelectron.* **2015**, *67*, 621–624.
28. Li, W.; Nie, Z.; He, K.; Xu, X.; Li, Y.; Huang, Y.; Yao, S. Simple, rapid and label-free colourimetric assay for Zn<sup>2+</sup> based on unmodified gold nanoparticles and specific Zn<sup>2+</sup> binding peptide. *Chem. Commun.* **2011**, *47*, 4412–4414.
29. Turkevich, J.; Stevenson, P.C.; Hillier, J. A study of the nucleation and growth processes in the synthesis of colloidal gold. *Discuss. Faraday Soc.* **1951**, *11*, 55.
30. Frens, G. Controlled nucleation for the regulation of the particle size in monodisperse gold suspensions. *Nat. Phys. Sci.* **1973**, *241*, 20–22.
31. Liu, J.; Lu, Y. Preparation of aptamer-linked gold nanoparticle purple aggregates for colourimetric sensing of analytes. *Nat. Protoc.* **2006**, *1*, 246–252.
32. Anwar, Z.M. *Complexation Equilibria of Zn(II), Pb(II) and Cd(II) with Reduced Glutathione (GSH) and Biologically Important Zwitterionic Buffers*; Chemical Society: Taipei, Taiwan, 2005; Volume 52, p. 9.
33. Lim, I.I.S.; Mott, D.; Ip, W.; Njoki, P.N.; Pan, Y.; Zhou, S.; Zhong, C.-J. Interparticle interactions in glutathione mediated assembly of gold nanoparticles. *Langmuir* **2008**, *24*, 8857–8863.
34. Beqa, L.; Singh, A.K.; Khan, S.A.; Senapati, D.; Arumugam, S.R.; Ray, P.C. Gold nanoparticle-based simple colourimetric and ultrasensitive dynamic light scattering assay for the selective detection of Pb(II) from paints, plastics, and water samples. *ACS Appl. Mater. Interfaces* **2011**, *3*, 668–673.
35. U.S. Environmental Protection Agency. *Definition and Procedure for the Determination of the Method Detection Limit-Revision 1.11*; 40 CFR Appendix B, Part 136; U.S. EPA: Washington, DC, USA, 2000.
36. Burns, C.; Spindel, W.U.; Puckett, S.; Pacey, G.E. Solution ionic strength effect on gold nanoparticle solution colour transition. *Talanta* **2006**, *69*, 873–876.
37. Basu, S.; Pal, T. Glutathione-induced aggregation of gold nanoparticles: Electromagnetic interactions in a closely packed assembly. *J. Nanosci. Nanotechnol.* **2007**, *7*, 1904–1910.

38. Wiegand, H.J.; Ottenwalder, H.; Bolt, H.M. The formation of glutathione-chromium complexes and their possible role in chromium disposition. In *Receptors and Other Targets for Toxic Substances*; Chambers, P., Cholnoky, E., Chambers, C., Eds.; Springer: Berlin, Germany, 1986; Volume 8, pp. 319–321.
39. Pietrzyk, D.J.; Frank, C.W. *Analytical Chemistry*; Academic Press: New York, NY, USA, 1979.
40. Penciner, J.S. *Stability Constants of Metal Complexes of 5-Sulfosalicylic Acid*; University of Toronto: Toronto, ON, Canada, 1962.
41. Sigel, H. *Metal Ions in Biological Systems. Volume 18: Circulation of the Metals in the Environment*; Taylor & Francis: New York, NY, USA, 1984.
42. Harris, D.C. *Quantitative Chemical Analysis*; W.H. Freeman: New York, NY, USA, 1999.
43. Krezel, A.; Bal, W. Coordination chemistry of glutathione. *Acta Biochim. Polonica* **1999**, *46*, 567–580.
44. Zhao, C.; Zhong, G.; Kim, D.-E.; Liu, J.; Liu, X. A portable lab-on-a-chip system for gold-nanoparticle-based colourimetric detection of metal ions in water. *Biomicrofluidics* **2014**, *8*, 052107.

© 2015 by the authors; licensee MDPI, Basel, Switzerland. This article is an open access article distributed under the terms and conditions of the Creative Commons Attribution license (<http://creativecommons.org/licenses/by/4.0/>).